BULLETIN OF THE EARTHQUAKE
RESEARCH INSTITUTE
Vol. 45 (1967), pp. 973-995

50. *Frequency Analysis of Seismic Waves (2).*

By Masaru TSUJIURA,

Earthquake Research Institute.

(Read April 25, 1967.—Received Sept. 30, 1967.)

Abstract

A seismic analyzing system of analogue type is constructed for the study of teleseismic signals which are recorded by magnetic tape recorders. The system is useful for 1) increasing the detectability of arriving seismic signals, 2) detecting mantle surface waves and measuring their arrival times, and 3) obtaining the frequency spectra of body waves of distant earthquakes.

The results of the analysis of the data obtained by the observations since April, 1966 can be summarized as follows.

1) High-pass and band-pass filterings are useful for detecting weak teleseismic *P* wave signals. 2) The low-pass filtering is also useful for detecting long-period mantle surface waves masked by short-period crustal surface waves and interfering waves, etc.. The arrival time of the surface waves can be measured by the use of the double filtering method. 3) The output signals of the multi-channel band-pass filters give the amplitude spectra of seismic waves, from which the relation between the predominant period of *P* waves and magnitude, and also the relation between the predominant period and focal depth for a certain magnitude range are obtained.

1. Introduction

Seismic data of analogue form recorded on magnetic tapes make it possible to perform rapidly and efficiently a wide variety of analyses, although the digital method is superior to the analogue one in accuracy. From this point of view, various technical procedures and studies on seismic waves have been achieved by Sutton and Pomeroy (1963)[1], Birtill and Whiteway (1965)[2], Wagner (1965)[3], and Sumner (1967)[4].

1) G. H. SUTTON and P. W. POMEROY, "Analog Analyses of Seismograms Recorded on Magnetic Tape," *J. Geophys. Res.*, **68** (1963), 2791-2815.
2) J. W. BIRTILL and F. E. WHITEWAY, "The Application of Phased Arrays to the Analysis of Seismic Body Waves," *Phil. Trans. Roy. Soc. London A*, **258** (1965), 421-493.
3) C. A. WAGNER, "Analog Event Detectors," Semiannual Technical Summary, Lincoln Laboratory, *M. I. T.*, ESD-TDR-65-597 (1965), 33-35.
4) R. D. SUMNER, "Attenuation of Earthquake Generated *P* Waves Along the Western Flank of the Andes," *Bull. Seism. Soc. Amer.*, **57** (1967), 173-190.

In my previous paper (1966)[5], spectral study of seismic signals were carried out by using an automatic processing device for spectral analysis connected to a short-period seismograph. The purpose of the present paper is to develop a wide variety of analyzing methods. The frequency range of original data for analysis is extended by the use of three kinds of seismographs, i.e., short, medium and long-period seismographs. All of them are recorded on magnetic tapes.

The principal idea of the analysis is to apply high-pass, low-pass and multi-channel band-pass filtering independently according to the object of the analysis. These include: 1) enhancement of the signal to noise ratio for various seismic waves by use of analogue filters; 2) measurement of arrival times of signals by eliminating the phase shift caused by the filtering; 3) determination of the amplitude and power spectra of various phases; and 4) conversion of the analogue data to digital data. These seismic data processings are routinely performed at our laboratory. Our future plan includes the construction of ultra long-period seismographs and the analysis of the records by the same method.

2. Observation equipment

Our instrumentation for the frequency analysis consists of the following elements.

a) Seismometers

In order to analyze seismic waves for a relatively wide frequency range, three kinds of seismometers, i.e., short, medium (two types) and long-period ones are used. The operating periods of these seismometers are 1 sec for the short-period, 4 and 20 sec for the medium-period and 15 sec for the long-period instrument.

b) Preamplifiers

The transducer of seismometers is of moving coil type. Since the output voltage of these transducers is small, preamplifiers are necessary. The gains of the amplifiers for the short-period seismometer are 80 db and 60 db for high and low magnifications respectively. Each amplifier has a flat frequency response over the range from 0.2 to 10 cps. Two medium-period preamplifiers are used, one is a mechanical chopper type DC amplifier with a flat 66 db voltage gain for the frequency range lower than 1 cps, and the other has a 66 db voltage gain for the fre-

5) M. TSUJIURA, "Frequency Analysis of Seismic Waves (1)," *Bull. Earthq. Res. Inst.*, **44** (1966), 873-891.

quency range from 0.2 to 10 cps. The response of the long-period preamplifier is similar to the medium-period one with the flat frequency response but the voltage gain is 100 db.

c) Prefilter

The prefilter, which consists of a two stage R-C low-pass filter[6], is inserted between the long-period transducer and the preamplifier to equalize the characteristics of our device to those of the world-wide standard long-period seismograph (15–90 sec).

d) Telemetering system

In order to attain a high magnification of the seismograph and also to increase the efficiency and accuracy of the observation, a radio tele-recording system of the seismograph is used. The main feature is as follows.

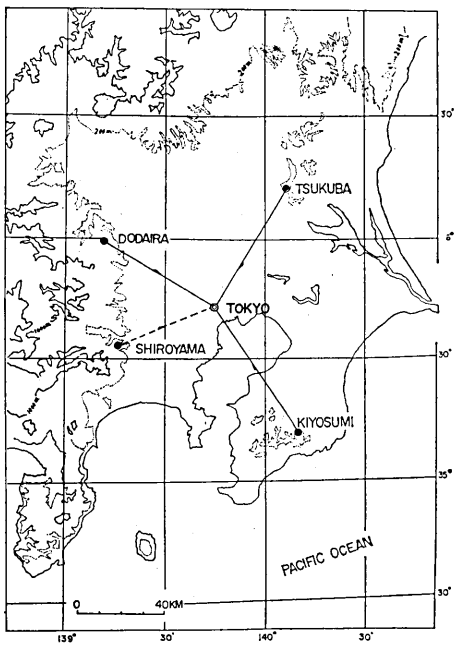

Fig. 1. Location of radio tele-recording seismic station.

The output signals of amplifiers are frequency modulated (FM) and converted to audio frequency signals. These audio frequency signals are sent to the receiving station at our Institute in Tokyo by the radio tele-recording system (RTS-II)[7,8].

Since the beginning of 1966, a new tele-recording system (RTS-III) has been added. The degree of the frequency modulation of RTS-III is $\pm 30\%$ for the short-period, and $\pm 50\%$ for the medium and long-period components. Fig. 1 gives the transmitting stations (seismological observatories) operating at present. Table 1 also shows the location of these seismological stations and its seismograph components.

6) M. TSUJIURA, "A Pen-Writing Long-Period Seismograph. Part 3," *Bull. Earthq. Res. Inst.*, **43** (1965), 429–440.

7) S. MIYAMURA and M. TSUJIURA, "UHF Multi-channel Radio Tele-recording Seismograph. Part 1," *Bull. Earthq. Res. Inst.*, **35** (1957), 381–394.

8) M. TSUJIURA and S. MIYAMURA, "UHF Multi-channel Radio Tele-recording Seismograph. Part II," *Bull. Earthq. Res. Inst.*, **37** (1959), 193–206.

Table 1. List of seismic stations.

Stations	Location	Elevation (m)	Rock type	Seismographs
Dodaira (DDR)	35° 59′ 54″.0N 139° 11′ 36″.2E	800	Paleozoic chert	Short, Medium, Long-period
Tsukuba (TSK)	36° 12′ 39″.0N 140° 06′ 35″.0E	280	Granite	Short, Medium-period
Kiyosumi (KYS)	35° 11′ 51″.6N 140° 08′ 53″.6E	230	Tertiary shale	Short, Long-period

At the receiving station, the radio frequency carrier is removed by a frequency demodulator. The audio frequency signals from each seismometer are processed independently, and are recorded routinely on magnetic tape recorders.

e) Magnetic tape recorder

Two types of magnetic tape recorder are used. One is for the short-period components and the other is for the medium and long-period components. Both of them have fourteen tracks with 1 inch width tape. The short-period tape recorder is equipped with an endless tape recording system and a storing system. The cycle time of the endless tape recording is adjusted to the duration of seismic signals. At present we set the cycle time of one loop at 40 sec. The recording tape of the storing system is controlled by a trigger system[9] that operates only at the time when earthquake signals arrive. The wow-flutter is less than 0.4% RMS when both systems are operated normally. Present tape speed is 3 3/4 ips (9.5 cm/sec) and recording time of the storing magnetic tape is about 60 sec for one earthquake.

For practical reasons, the long-period magnetic tape recorder is operated continuously at the tape speed of 15/16 ips (2.38 cm/sec). One reel per day is necessary when we use a 14 inch reel and a tape length of 7200 feet. The wow-flutter is 0.5% RMS and the signal-to-noise ratio is 40 db.

f) Visible recorder

The audio frequency (subcarrier) outputs are also discriminated by frequency demodulators to reproduce seismic signals.

These signals are recorded on visible monitor recorders in parallel with the magnetic tape recording. The short-period recorders consist of

9) M. TSUJIURA, "Multi-Channel Triggered Magnetic Tape Recording for Routine Seismic Observation. Part 1," *Bull. Earthq. Res. Inst.*, **41** (1963), 419-445.

a drum and four channel ink-recording oscillograph. The oscillograph record of four stations on the same recording paper is used not only for phase identification but also for determining accurate arrival times.

For the medium-period, a drum recorder which is equipped with a band rejection notch filter is used to suppress the microseisms. An automatic balanced type drum recorder (Helicorder) and three pen chart recorders are used as the long-period recorders. These records provide a permanent visible record and, at the same time, monitor the long-period instruments and magnetic tape outputs.

3. Magnification curve

Fig. 2 shows the standard magnification curves of seismographs

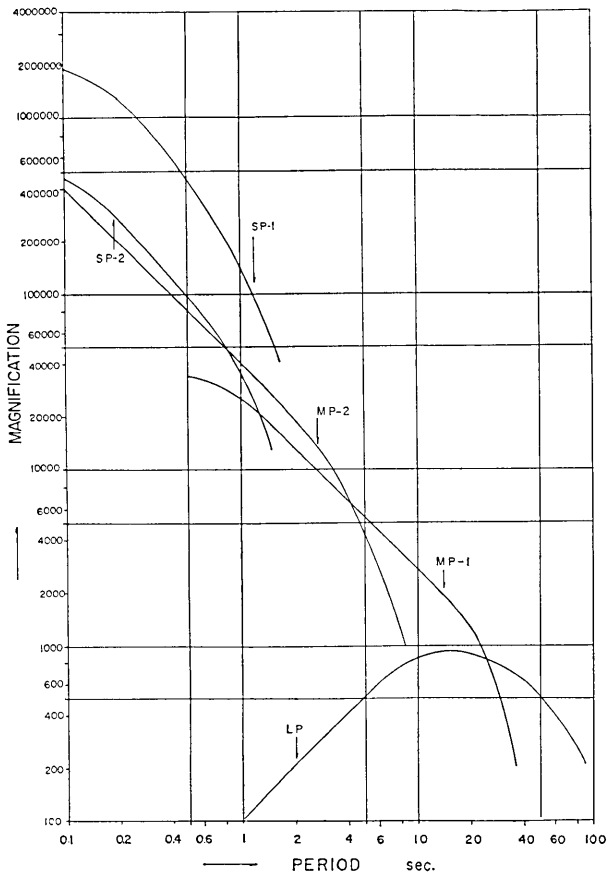

Fig. 2. Magnification curves of the seismographs.

used in the analysis. LP indicates the characteristics of long-period seismographs operated at Dodaira (DDR) and Kiyosumi (KYS) stations. MP-1 and MP-2 also indicate the characteristics of medium-period seismographs operated at Tsukuba (TSK) and DDR stations respectively. SP-1 indicates the characteristics of a high magnification short-period seismograph operated only at the TSK station. SP-2 indicates the characteristics of the low magnification short-period seismographs at TSK and the other two stations.

4. Analyzing equipment

A flow chart of the data analysis facility is shown in Fig. 3. The magnetic tape seismogram is reproduced at the desired speed by the reproducing tape machine. The resulting signal can be analyzed in the analogue form directly. Each unit of the frequency analysis facility is explained in the following.

a) Reproducing magnetic tape recorder

The reproducing magnetic tape recorder is the same as that for recording except that it has a range of tape speeds. It can be operated at the ordinary tape speed and, in addition, at two and eight times the ordinary speed. The length of the analysis time can be shortened by speeding up the reproducing tape. However, the upper limit of tape speed depends on the frequency response of the analyzer or the time rate of the A/D converter. At present the higher limit of the frequency analyzer is 30 cps, as will be described in the next section. Therefore, eight times the ordinary tape speed is the upper limit if we take 4 cps as the upper frequency which may be contained in teleseismic body waves.

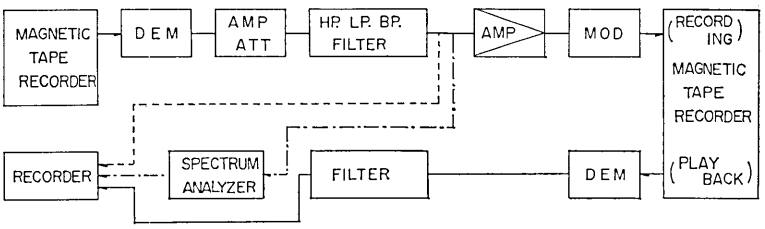

Fig. 3. Block diagram of the analogue frequency analysis facility.

DEM: Demodulator
AMP: Amplifier
ATT: Attenuator
MOD: Modulator
HP: High-pass
LP: Low-pass
BP: Band-pass

b) Amplifier or attenuator

The dynamic range of our analogue frequency analyzer is narrower than that of the seismographs. Therefore, an amplifier or attenuator is equipped before the analyzer.

The amplifier is a DC amplifier with a transistor chopper and the frequency response is from DC to 4 cps and is flat within 3 db. In order to obtain the proper amplitude for the analyzed data the gain of the amplifier is adjusted to between +20 to −12 db according to the amplitude of the original records.

c) Filter

High-pass (HP), Low-pass (LP) and Band-pass (BP) filters are used for the frequency analysis of seismic data. The high-pass or band-pass filter is used to improve the signal to noise ratio of *P* waves masked by the microseisms and other noises. The high-pass filter has corner frequencies of 0.5 and 1.0 cps and an attenuation slope of 40 db/octave. The multi-channel band-pass filter, manufactured by Tateishi Electronic Co., is separated into 11 channels covering the period range of 0.03 to 60 sec. The pass-band has one octave width between −3db points and an attenuation slope of 40db/octave for each filter, as is shown in Fig. 4 for example. Table 2 shows the band width of each channel of the filter. These are useful not only for detecting *P* or any other phases but also for identi-

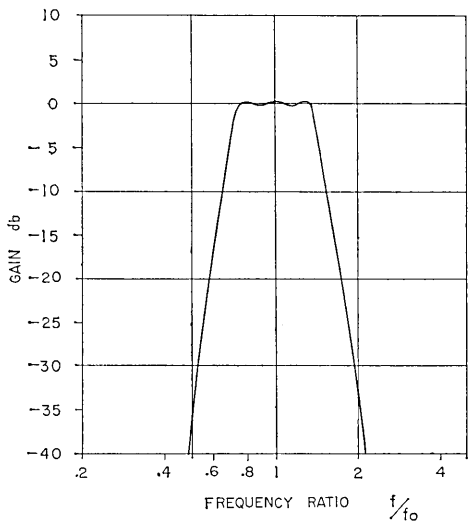

Fig. 4. Typical frequency characteristic of band-pass filter.

Table 2. Band width and channel number of band-pass filters.

CH	1	2	3	4	5	6	7	8	9	10	11
BW	60.0	29.5	15.5	8.0	3.7	1.9	0.92	0.46	0.23	0.12	0.06
(sec)	31.0	15.5	8.0	3.8	1.9	0.95	0.48	0.24	0.12	0.06	0.03
BW	0.0167	0.0341	0.0645	0.125	0.271	0.526	1.08	2.18	4.35	8.35	16.7
(cps)	0.0323	0.0645	0.125	0.263	0.526	1.05	2.08	4.18	8.35	16.7	33.3

fying various phases on the basis of the frequency-amplitude spectrum.

In order to obtain the spectral distribution of the energy in body waves, the spectrum analyzer is used. The analyzer is combined with these eleven band-pass filters and eleven integrators which can integrate for arbitrary time intervals. The procedure can be summarized as follows. We denote the frequency-amplitude characteristic and frequency-phase characteristic of the seismograph by $U(\omega)$ and $\gamma(\omega)$ respectively, where ω is the angular frequency. Then, the spectrum of the seismogram $Y(\omega)$ is given by

$$Y(\omega)=X(\omega)\,U(\omega)e^{i\gamma(\omega)},$$

where $X(\omega)$ is the spectrum of the ground motion.

In order to obtain the spectrum of seismic signals, the signal is passed through the multi-channel band-pass filter. The output signal of the i-th channel band-pass filter is given by

$$y_i(t)=\int_{-\infty}^{+\infty}X(\omega)\,U(\omega)e^{i\gamma(\omega)}F_i(\omega)e^{i\omega t}d\omega\,, \qquad (1)$$

where $F_i(\omega)$ is the frequency response of the i-th channel. From these we can obtain the spectrum of the seismic wave.

Low-pass filters with corner periods of 10, 20, 40 and 60 sec, and with an attenuation slope of 36 db/octave for each filter are used. This is effective for the detection of long-period surface waves (mantle surface waves) masked by crustal short-period surface waves. However, when the original signal is passed through the filter it undergoes a frequency dependent phase shift. For the determination of the arrival time of a particular phase it is more convenient if the phase shift can be compensated.

The method of phase compensation is illustrated by the solid line in Fig. 3. The original magnetic tape seismogram, after being passed through a given filter, is re-recorded on another magnetic tape, as shown by the upper solid line in the figure.

By now, both amplitude and phase spectrums of the original record are affected by the filter. In the next procedure, the re-recorded tape is reversely (from the end to the beginning) passed through the same filter and recorded on a visible recorder as indicated by the lower solid line in the figure. By this procedure the amplitude response of the filter is squared but the phase shift is completely cancelled. More precisely, we can write the above procedure as follows. We will

write the frequency spectrums of the input signal and the filter as $a(\omega)\exp\{i\theta(\omega)\}$, $b(\omega)\exp\{i\phi(\omega)\}$ respectively. Then the once-filtered signal can be given by

$$a(\omega)b(\omega)e^{i\{\theta(\omega)+\phi(\omega)\}}.$$

To play back the tape in the reverse direction is equivalent to changing the sign of the time which is, in the frequency domain, equivalent to changing the sign of the phase angle. Hence, if we again pass the tape reversely through the same filter, we have as the output,

$$a(\omega)b(\omega)e^{-i\{\theta(\omega)+\phi(\omega)\}}b(\omega)e^{i\phi(\omega)}=a(\omega)b^2(\omega)e^{-i\theta(\omega)}.$$

By looking at the output reversely, we can change the sign of the phase angle. Thus, the signal has been multiplied by the square of the filter amplitude characteristic, but the original phase angle is preserved.

d) Recorder

A three pen chart recorder and a twelve channel ink-recording oscillograph are used for the presentation of the analyzed data.

e) On-line spectrum analyzer

For the short-period components, the magnetic recording methods with the trigger system are used as mentioned before.

The trigger level is decided after due consideration of the amplitude of microseisms, the ground noises and the seismicity of near earthquakes. However, when the seismicity is very high, the trigger level can be set at the lower level so as to limit the number of data. In such a case, small teleseismic events cannot be recorded on our magnetic tape. As reported in Part 1[10] of this study, the automatic processing spectrum analyzer is constructed and operated routinely to record those small teleseismic signals.

f) A/D converter

Seismic signals on magnetic tapes are converted to digital form on paper tapes by use of an analogue to digital converter (Hitachi Hidas-5100). This unit operates at a maximum rate of 500 samples per second.

5. Result of frequency analysis

One of the highest merits of magnetic tapes is that they can be used for repeated reproduction of the recorded signal.

10) *loc. cit.*, 5)

Some results obtained by the procedure mentioned above are shown in the next paragraph.

1) Detection of weak teleseismic waves

The practical procedure is as follows. The signal from the magnetic tape recorder is amplified and reproduced directly without any filtering on a visible recorder. If some suspicious motions can be found in the records, the low-pass, high-pass or band-pass filters are used to identify these motions. Usually, strong microseismic signals are superposed upon the small teleseismic waves. However, the band width of the spectrum of the seismic wave may be broader than that of the microseismic signals though the detailed spectrum of the seismic signal is as yet unknown. Therefore, the signal-to-noise ratio in the channels outside the band width of microseismic signals can be improved by the filtering. For example, Fig. 5 shows the result of filtering for the Central Mid-Atlantic ridge earthquake of Jan. 24, 1967, recorded by the medium-period seismograph at Tsukuba. The hypocenter data for this earthquake

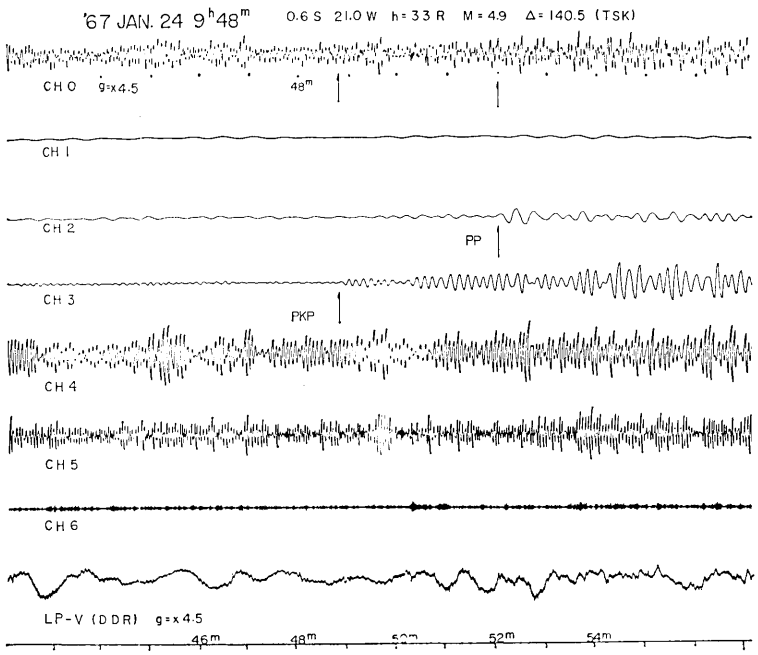

Fig. 5. An example of detection of weak teleseismic signals by use of band-pass filtering. The value of the focal depth with R is a restrained one.

and all other events in this paper were obtained from the PDE cards of USCGS.

The top trace designated by CH 0 is the original seismogram without any filtering. The CH numbers from 1 to 6 indicate the channel number of the band-pass filters. The frequency range and band width of the filter are given in Table 2. The magnification of the amplifier for the analysis is about 4.5 times the standard magnification curve (MP-1) in Figure 2. But the magnification of the original record (CH 0) is about 1/3 of that of the filtered ones so as to keep the power amplifier for the recording galvanometer from saturating. Large microseismic signals make it difficult to identify any phase in the original record (CH 0). However, two phases, *PKP* and *PP*, are easily found on the records of CH 2 and CH 3 since the microseisms which appear in channels CH 4 and CH 5 do not disturb these channels. The Jeffreys-Bullen residual of the *PKP* phase given by USCGS based on our regular report is +0.6 sec. The bottom trace shows the long-period vertical seismogram recorded at Dodaira for which the magnification is 4000 at the period of 10 sec. We could not find any phase from this record because long-period ground noises are too large.

Generally, the predominant period of microseisms is 3 to 8 sec. However, the higher harmonics of microseisms below 3 sec exist, and these short-period microseisms limit the magnification of short-period seismographs. One of the possible methods of rejecting microseisms is to use velocity filtering[11] i.e., Delay-and-Sum or Filter-and-Sum of the signals from an array station. However, for the single station, the high-pass filtering which has a corner period of 1 or 2 sec is also effective to reject these microseisms. The signal-to-noise ratio can be especially improved for deep earthquakes since they are abundant in short-period components. Considering these, at KYS station where the detection capability is lower than that at the other stations because of the proximity to the Pacific Ocean, the high-pass filtering is routinely operated.

Fig. 6 shows the sample of the original and the record through the high-pass filter. Both are from the same short-period vertical seismograph set up at KYS. As is seen in this figure, the signal-to-noise ratio is considerably improved.

The J-B travel time residual of the *P* phase in this record is −2.2 sec.

11) *loc. cit.*, 2)

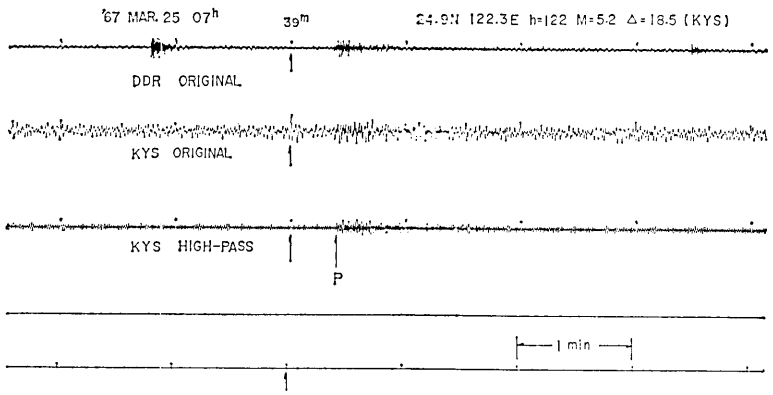

Fig. 6. An example of detection of teleseismic signals by use of high-pass filtering.

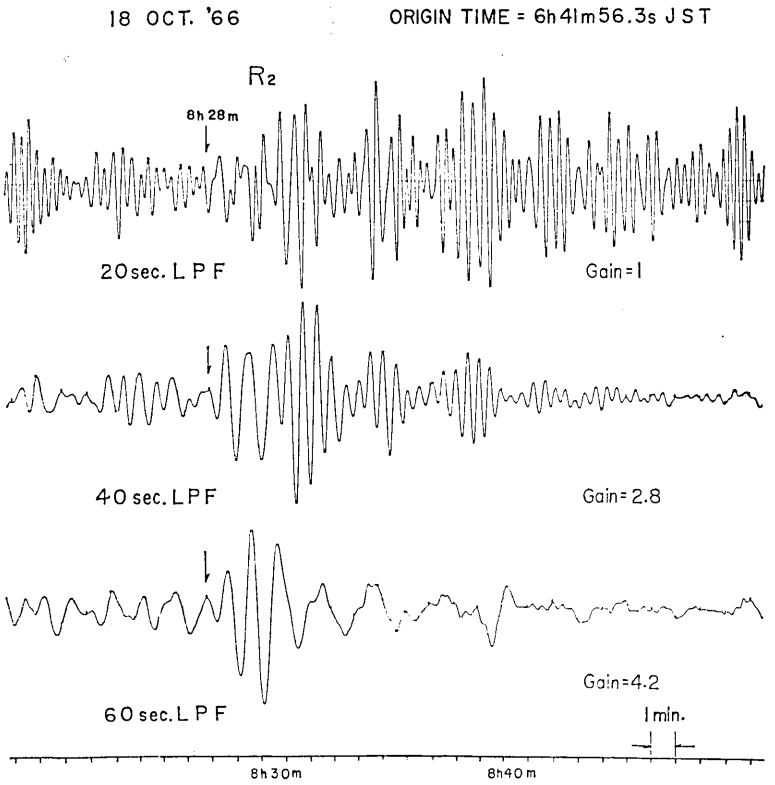

Fig. 7. An example of detection of mantle Rayleigh wave by use of low-pass filtering. (JST=GMT+9 h).

The determination of the spectrum of surface waves is quite important, because it depends not only on the nature and the dimension of the source, but also on the character of the dispersion. Therefore, in the first stage, we examined the existence of long-period (mantle) surface waves for large earthquakes observed at our station. Usually mantle surface waves, such as $G1$, $R1$, $G2$ and $R2$, are superposed upon by short-period crustal surface waves and some interfering waves. Then, we used the low-pass filtering to detect these waves. The low-pass filters have corner periods of 10, 20, 40 and 60 sec, and the attenuation slope is greater than 36 db/octave for each filter.

Fig. 7 shows the result of the filtering for the near coast of Peru earthquake of Oct. 17, 1966, recorded by the long-period seismograph at KYS. The records from the top to the bottom are through the low-pass filters which have the cut off period at 20, 40 and 60 sec respectively. The bottom trace clearly shows the inverse dispersion of the mantle Rayleigh wave.

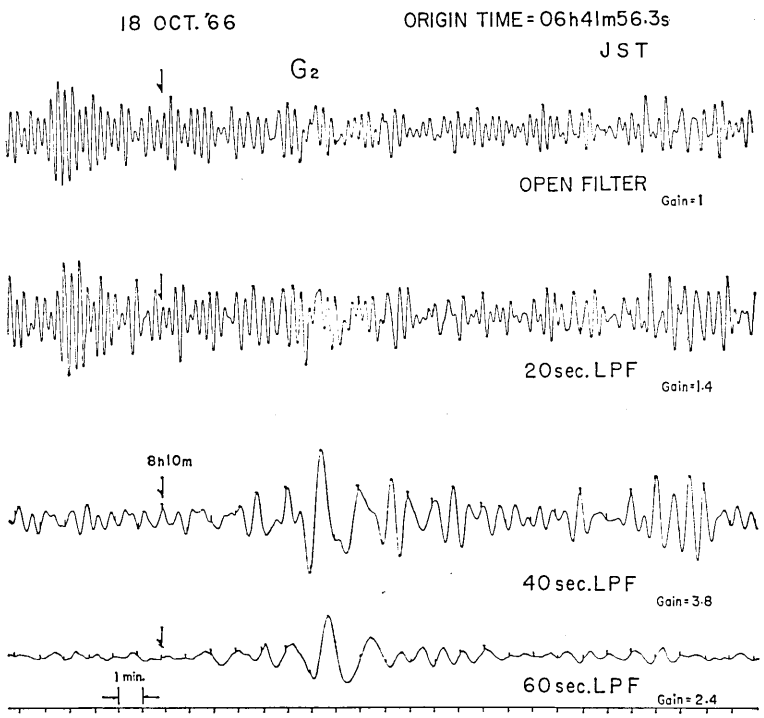

Fig. 8. An example of detection of mantle Love wave by use of low-pass filtering. (JST=GMT+9 h).

The same method is used for Love or G waves. Fig. 8 shows the $G2$ wave train from the same earthquake. The pulse-like nature of the long-period component of the G wave is clearly demonstrated by the low-pass filtering. These techniques are effective to measure the group velocity and also the phase velocity by use of wave train combinations such as $G1$-$G3$, $R1$-$R3$, $G2$-$G4$, $R2$-$R4$, etc.. This problem will be discussed below.

2) Measurement of arrival time of various phases

In the case of measuring the arrival time or group velocity of the seismic waves by the use of analogue filtering, the phase shift caused by the filtering must be compensated in order to know the actual phase angle of the original records. The phase shift is compensated by the double filtering method.

Fig. 9 shows the result of the double filtering. The top trace is the original seismogram given in Fig. 7. The middle trace is also the same as the bottom trace of Fig. 7. The bottom trace, indicated as fi-1, shows the result of double filtering which compensates the phase shift of the filter. As is seen in this figure the position of the peak of the middle trace is about 22 sec later than that of the bottom trace.

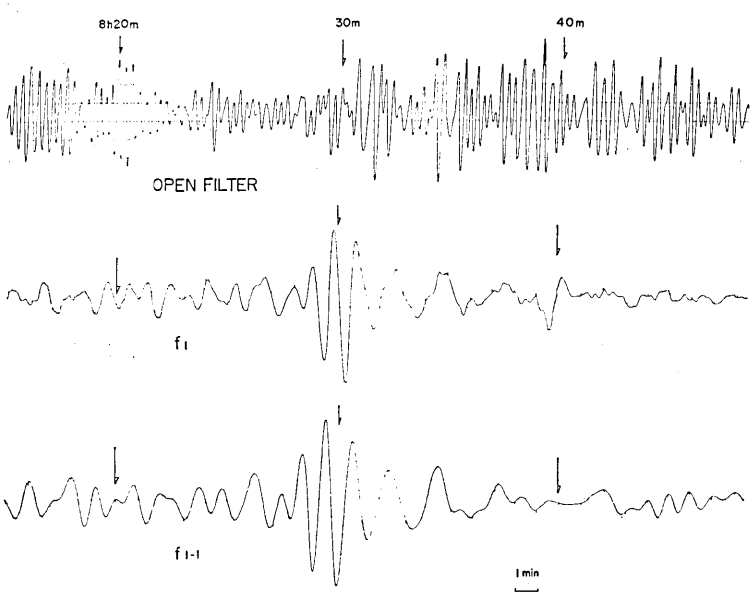

Fig. 9. An example of phase shift compensated filtering.

This effect is caused by the filtering. The group velocity of the wave can be measured more accurately from the bottom record.

3) Amplitude spectra of various phases of seismic waves

The present method is useful to study the dependence of the frequency spectrum of seismic waves on magnitude, epicentral distance, ray paths and mechanism of occurrence. We analyzed, a) the spectrum of P wave from the various earthquakes, and b) the amplitude ratios of P to PcP and P to PP or to S waves, etc., at various frequencies for a given earthquake. The analysis will enable us to obtain information of the frequency spectrum at the source and the attenuation factor of the medium. From this point of view, we investigated at first how the spectra of P and other phases depend on the magnitude, focal depth and the epicentral distance.

There are several ways to perform spectral analysis by the digital Fourier technique, as reported by Matumoto (1960)[12] and others. However, the analogue method is easier than the digital one to analyze a great deal of data. The block diagram of our method is shown in Fig. 3. This analyzer provides 11 band-pass filters (and 11 integrators with common time control units). The procedure of the analysis is as follows: the seismograms passing through the band-pass filters are recorded on a visible twelve channel ink-recording oscillograph together with the original record.

Fig. 10 shows the analyzed data from the long-period seismograph at DDR. The top trace is the original record from the magnetic tape. The second trace indicated as CH 0 (channel number 0) is the same as the top trace except for the recording equipment. For a better display of the filtered traces, the gain of the amplifier for the analyzer is changed before the S phase arrival, as shown in Fig. 10. CH 1-CH 6 are the outputs from the band-pass filters where the numbers 1-6 are the channel numbers. Records from CH 7 to 11 are not shown since the signal has no components in these channels. The analyzed data show that different phases have different spectra. The short-period components of later phases are usually more strongly attenuated than those of the first arrival. However, two minutes after the initial onset, a clear phase is found in the short-period channels which is identified as the PP or PcP phase from the travel time table. Considering our result that the PcP phase usually has large short-period components, this phase may

12) T. MATUMOTO, "On the Spectral Structure of Earthquake Waves. —The Relation between Magnitude and Predominant Period—," *Bull. Earthq. Res. Inst.*, **38** (1960), 13-27.

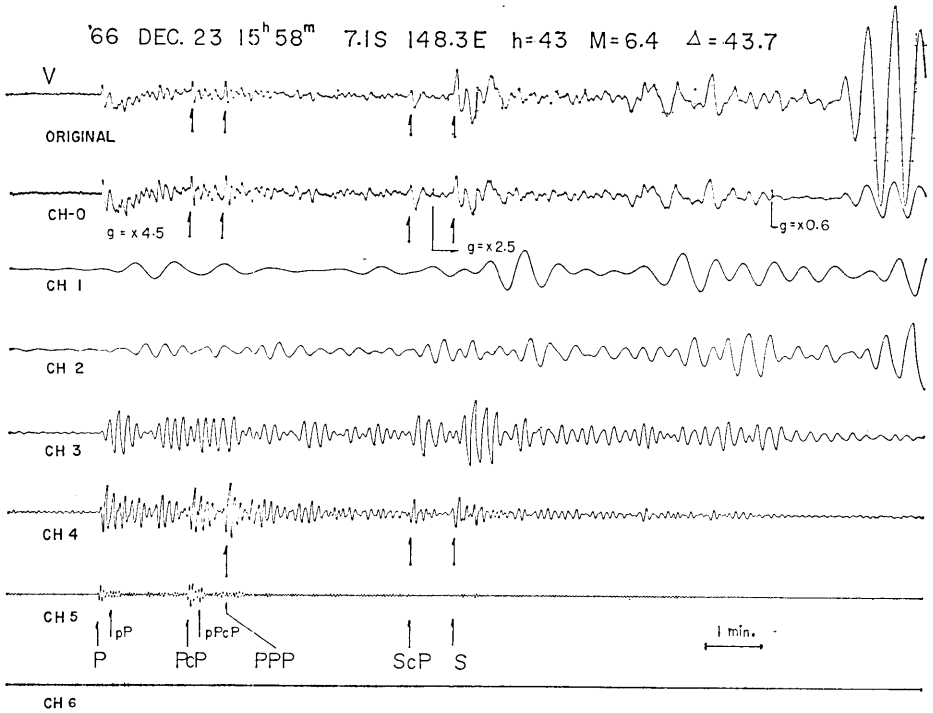

Fig. 10. An example of the frequency-analyzed data for the long-period vertical component.

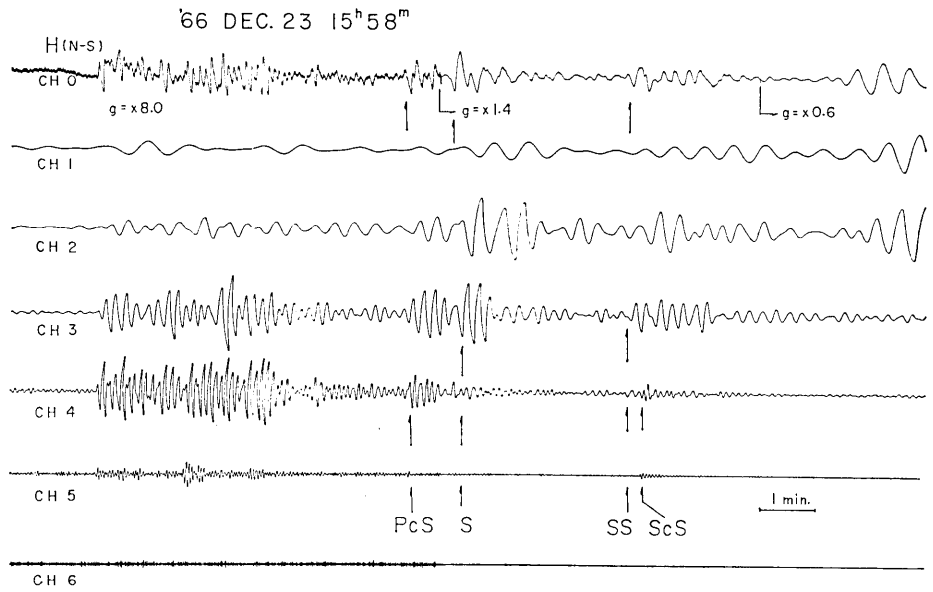

Fig. 11. An example of the frequency-analyzed data for the long-period horizontal component.

be identified as *PcP*. The amplitude spectrum of various phases can be approximately obtained from the data. Consulting it, we can identify various phases by the general appearance of the filtered outputs. Fig. 11 also shows the analyzed horizontal component record of the same earthquake as illustrated in Fig. 10. Phases indicated by arrows are clearly shown in the filtered traces. A clear *ScS* phase can be found in the short-period channels of CH 4 and CH 5. The *ScS* phase is more abundant in short-period components than is the *ScP* phase. It may be suggested that *S* to *P* conversion at the core boundary undergoes a stronger attenuation than does *S* to *S* conversion and loses high frequency components.

We analyzed earthquakes at various epicentral distances. Table 3 shows the epicenter locations of these earthquakes. However, not so many earthquakes have clear later phases. Therefore we first studied the amplitude spectra of *P* waves. Amplitudes and periods of *P* with a relatively large signal-to-noise ratio were read from the analyzed data of each seismograph set up at the three stations, and the corresponding

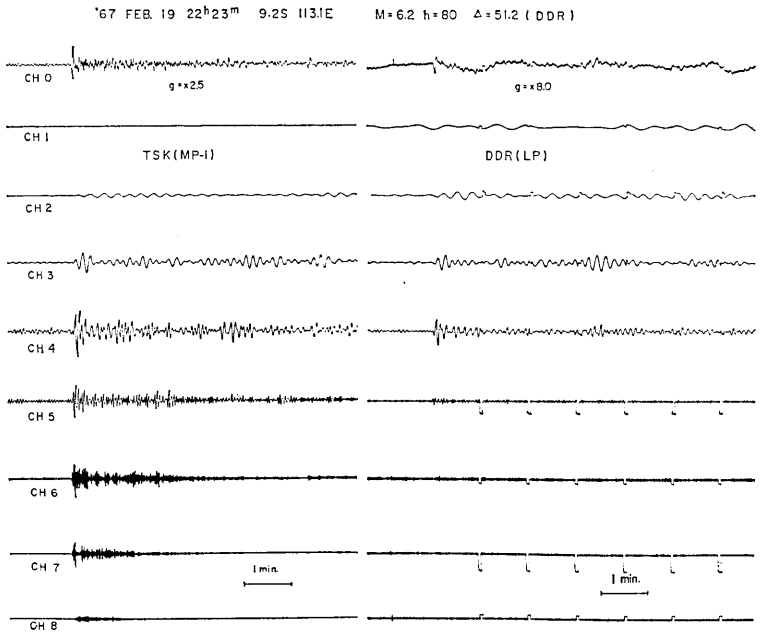

Fig. 12. Comparison of medium-period seismogram at TSK with long-period seismogram at DDR station.

Table 3. List of earthquakes and the

No.	Date 1966	Origin time G. M. T.	Location	Depth (km)	Magnitude CGS
		h m s			
1	June 15	00 59 45.8	10.4S 160.8E	31	6.1
2	July 21	03 57 57.8	49.7N 77.9E	0R*	5.6
3	Aug. 19	12 22 09.6	39.2N 41.7E	26R*	6.1
4	Dec. 1	04 56 58.2	14.0S 167.1E	132	6.1
5	Dec. 14	03 44 01.9	52.9N 177.6W	243	5.3
6	Dec. 16	20 52 13.5	29.6N 81.0E	9	5.9
7	Dec. 21	08 52 00.2	20.0S 169.7E	245	5.6
8	Dec. 23	15 50 20.4	7.1S 148.3E	43	6.4
9	Dec. 31	18 23 03.9	11.8S 166.5E	33R*	7.7**
10	Dec. 31	22 15 14.0	11.3S 164.8E	33R*	7.3**
	1967				
11	Jan. 5	00 14 40.4	48.1N 102.8E	33R*	6.4
12	Jan. 18	05 34 32.6	56.6N 120.8E	11	6.1
13	Jan. 18	08 18 22.0	52.5N 168.3W	37	5.7
14	Jan. 19	12 38 31.3	11.8S 166.4E	156	5.5
15	Jan. 19	12 40 12.6	14.8S 178.8W	18	6.6
16	Jan. 20	01 57 23.1	48.0N 102.9E	33R*	6.1
17	Jan. 28	13 52 58.3	52.4N 169.5W	47R*	6.7**
18	Feb. 7	08 28 57.9	13.9N 144.8E	138	5.4
19	Feb. 17	10 10 51.5	23.7S 175.2W	19	6.4
20	Feb. 19	22 14 35.3	9.2S 113.1E	80	6.2
21	Feb. 19	23 28 28.0	0.0S 124.2E	101	5.7
22	Feb. 22	18 26 46.7	19.5S 169.0E	87R*	5.6
23	Feb. 25	11 20 47.4	0.0S 123.9E	70	5.8
24	Feb. 25	11 38 46.0	0.1S 123.9E	105	5.7
25	Feb. 26	03 57 57.7	49.8N 78.1E	0R*	6.0
26	Mar. 2	23 03 39.7	53.8N 160.5E	21	5.0
27	Mar. 4	06 16 21.9	18.5S 175.4W	225R*	5.7
28	Mar. 4	17 58 06.4	39.2N 24.6E	33R*	5.9
29	Mar. 9	06 58 35.7	10.6S 166.3E	30	6.0
30	Mar. 9	18 02 45.7	10.7S 166.3E	59	6.4
31	Mar. 11	08 33 27.4	10.7S 166.2E	49R*	6.1
32	Mar. 13	19 22 15.4	19.7N 38.9E	7	5.8
33	Mar. 14	06 58 04.6	28.4N 94.3E	24	5.9
34	Mar. 19	01 10 45.8	6.7S 129.9E	60	5.9
35	Mar. 24	09 00 19.5	6.0S 112.3E	600R*	6.0
36	Mar. 30	02 08 02.4	11.0S 115.5E	33R*	6.0
37	Apr. 8	05 35 17.1	19.9S 178.6W	616	5.3
38	Apr. 9	00 05 07.0	4.0S 135.8E	15R*	5.1
39	Apr. 9	08 56 59.7	7.2S 155.8E	40	5.1
40	Apr. 10	15 02 42.2	7.3S 155.8E	29R*	5.6
41	Apr. 12	04 51 40.2	5.3N 96.5E	55	6.1
42	Apr. 12	13 54 57.2	7.3S 155.6E	52	5.2
43	Apr. 12	14 51 49.4	7.4S 155.7E	21	5.3
44	Apr. 13	18 40 07.7	52.1N 157.0E	50R*	5.3
45	Apr. 20	04 07 57.6	49.7N 78.1E	0R*	5.7
46	Apr. 29	03 55 20.8	51.4N 178.3W	50	6.0

*: Restrained focal depth.
**: Surface wave magnitude.
***: Magnitude assigned by USCGS for TSK.
****: Phases identified by the spectral analysis and travel time. *P* and *S* phases are not mentioned here.

results of frequency analysis.

Magnitude*** TSK	Distance (degree)	Predominant period (sec)	Identified phase****	Region
—	50.3	11.0	—	Solomon Is.
—	46.2	0.5	—	E. Kazakh
—	73.8	7.0	—	Turkey
—	56.3	9.5	*PPP*	New Hebrides Is.
—	33.9	0.5	—	Aleutian Is.
—	49.4	6.4	—	Nepal
—	62.7	6.0	*ScS*	New Hebrides Is.
—	43.7	5.4	*PcP, PPP, ScP*	E. New Guinea
—	53.5	38.0	—	Santa Cruz Is.
—	52.7	20.0	—	Santa Cruz Is.
—	29.3	21.0	*PP, PcP*	Mongolia
—	24.1	6.0	*PP*	E. Russia
—	40.1	5.0	—	Aleutian Is.
—	54.1	5.3	—	Santa Cruz Is.
—	64.3	10.3	—	Fiji Is.
—	29.7	11.5	*PP, PPP, PcP*	Mongolia
6.1	39.3	20.0	*pP, PP*	Aleutian Is.
5.5	22.6	6.0	*PP*	Mariana Is.
6.2	73.3	10.0	—	Tonga Is.
6.4	51.2	5.0	—	Java
5.8	38.5	0.72	*PcP*	Molucca Sea
6.1	62.0	4.5	*pP, sP*	New Hebrides Is.
5.8	38.6	1.2	*PcP*	N. Celebes
5.5	39.1	1.1	*PcP*	N. Celebes
6.4	45.6	0.6	—	E. Kazakh
—	23.2	1.4	—	Kamchatka
6.2	69.1	5.0	*sP*	Tonga Is.
6.5	83.9	6.0	*PP*	Aegean Sea
—	53.0	10.0	*PcP, PP, ScS*	Santa Cruz Is.
—	53.0	6.0	*PcP, PP*	Santa Cruz Is.
6.1	53.0	5.5	—	Santa Cruz Is.
6.1	86.6	2.4	—	Red Sea
—	39.2	5.0	*PP, SS*	India-China
5.9	43.3	2.5	—	Banda Sea
—	48.8	10.0	*pP, PP*	Java Sea
5.8	51.8	6.5	*pP*	Bali Is.
5.5	68.4	2.5	*pP*	Fiji Is.
5.2	39.9	3.0, 6.5	—	W. New Guinea
6.1	45.7	1.4	—	Solomon Is.
6.2	45.8	1.5,12.0	*PP*	Solomon Is.
6.1	49.7	6.5	*X*	N. Sumatra
5.7	45.8	2.1	—	Solomon Is.
5.6	45.8	1.5	—	Solomon Is.
5.6	20.7	0.7	—	Kamchatka
6.1	46.1	0.55	—	E. Kazakh
—	34.1	1.4	*PcP*	Aleutian Is.

ground amplitudes in microns were calculated. From these results, the periods of the wave with the maximum amplitude in the vertical component of P are also listed in Table 3. Fig. 12 shows one of the analyzed data of body waves recorded at the two different stations. In this figure, the maximum amplitude is found in channel 4 (CH 4) for both records. When we take into account the overall magnification of the seismographs, we know that the predominant period is about 5 sec. However, if the predominant period of the record at one station is different from the other for a given earthquake, the data are rejected since the effect may be caused by the local effect at the stations. As can be seen in this table, the predominant period depends on the magnitude and focal depth. This problem will be discussed in the next section.

4) Relation between magnitude and predominant period

The results obtained by the procedure mentioned in the previous

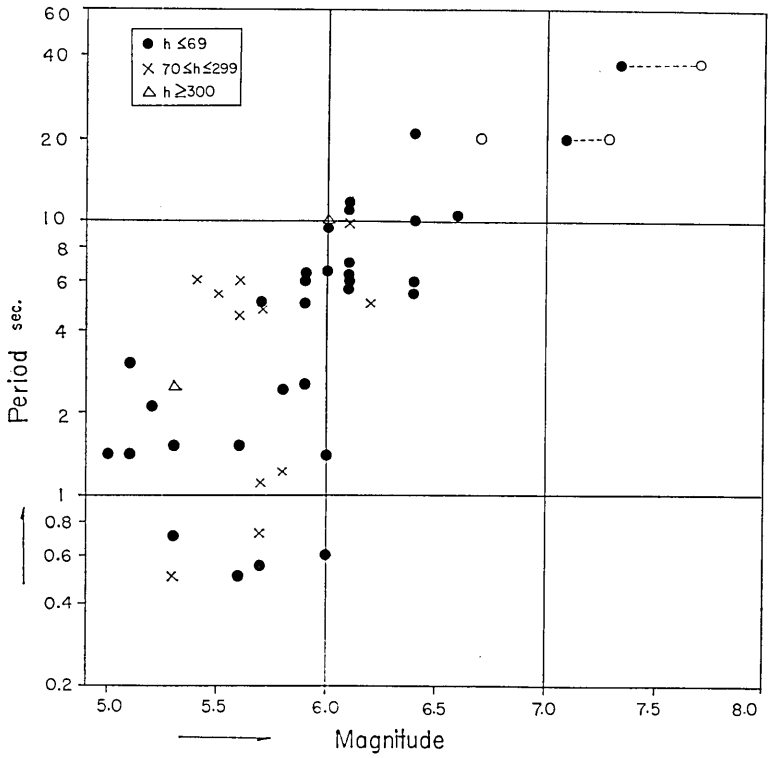

Fig. 13. Magnitude-Predominant period relation. Open circles correspond to surface wave magnitude in Table 3. If body wave magnitude is used, the open circles should be moved as shown in the figure.

section are shown in Fig. 13. As is seen in this figure, a close correlation exists between the period of seismic waves with maximum amplitude and the magnitude of the event. Generally speaking, the predominant period increases with increasing magnitude, as reported by Kasahara (1957)[13] and Matumoto (1960)[14]. However, the relation shown here is not as systematic as those reported by them. In this figure, the earthquakes are classified into three depth groups, i.e., 0-69 km, 70-299 km and deeper than 300 km. We did not classify for the epicentral distance since the distance of the earthquakes used here ranges from 20 to 90 degrees, over which the predominant period does not appreciably change. As is seen in this figure, a large scattering is found for the magnitude range less than 6.0. For example, as indicated by cross marks, the predominant period of about 1 sec is found for the earthquakes with focal depth of about 100 km in the Celebes and Molucca Sea regions, while the period of about 6 sec is found for the earthquakes with focal depth of about 200 km in the New Hebrides and Tonga Is. regions, although they have about the same magnitude. A period of about 0.5 sec is also found for the earthquake with focal depth of 250 km in the Aleutian Is. region. As reported by Gutenberg (1958)[15] and Tsujiura (1966)[16], the predominant period of P waves shifts to the shorter period range with increasing focal depth. However, from the result of this study, the influence of the regional difference on the predominant period of P waves seems to be greater than that of the difference in focal depth. It may be suggested that physical properties of the material near the source have much influence on the spectral structure of seismic waves, and that even if we eliminate the effect of epicentral distance and wave path, the regional effect on the predominant period will still survive.

Another interesting fact is seen for three events which occurred in the Kazakh region of Central Asia. The predominant period of these events is very short (0.5 sec) though they have shallow focal depth (0 km). Fig. 14 shows the analyzed data of one example of the three events as compared with two other events. All events occurred in the Eurasia region. The left traces show the Kazakh region event; the middle, the India-China border; and the right, the Aegean sea event. All events

13) K. KASAHARA, "The Nature of Seismic Origin as Inferred from Seismological and Geodetic Observations (1)," *Bull. Earthq. Res. Inst.*, **35** (1957), 473-532.

14) *loc. cit.*, 12)

15) B. GUTENBERG, "Attenuation of Seismic Waves in the Earth's Mantle," *Bull. Seism. Soc. Amer.*, **48** (1958), 269-282.

16) *loc. cit.*, 5)

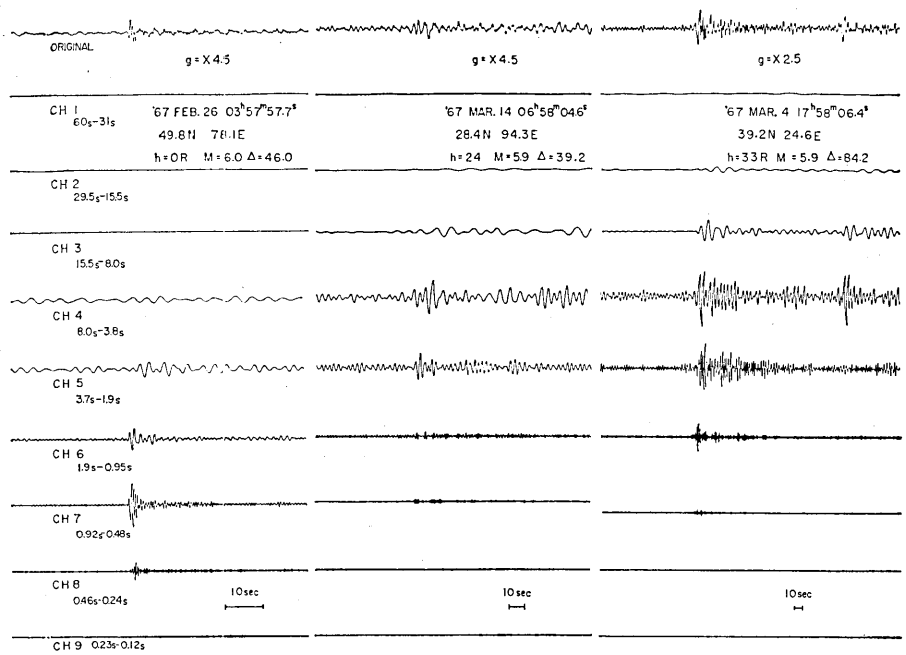

Fig. 14. An example of analyzed medium-period seismograms at TSK for three different teleseismic events. Note the different time scales!

have almost the same magnitude. However, as is seen in this figure, the band width of the spectrum and the predominant period of the Kazakh event are very different from those of the other events. If we assume that the predominant period of P waves is proportional to the source dimension, the spatial energy density at the source may be larger for the short period event such as the Kazakh event, than for ordinary events with the same magnitude. It would be interesting to study the regional variation of the predominant period of seismic waves and the relation between magnitude and predominant period. For this purpose, more spectral information of seismic waves from various seismic regions and focal depths will be very important.

6. Summary

The method presented in this paper is useful for the spectral analysis of seismic data in analogue form, because of its simplicity and rapidity of data processing. Therefore, the analysis can be made on routine

observations to accumulate a large amount of data for the statistical study of the seismic wave spectrum.

Acknowledgment

The writer wishes to express his thanks to Prof. Setumi Miyamura for his guidance and encouragement continuously given in the course of present study. The writer also thanks Drs. Hiroo Kanamori and Megumi Mizoue for their valuable advice. The staff of Dodaira seismological station gave the writer kind help for the observations.

---

50. 地震波動の周波数分析 (2)

地震研究所　辻　浦　賢

High-pass, Low-pass, Band-pass 等3組の Analog filter をもちい，Magnetic tape にためこまれた地震記象の周波数分析をおこなった．

1966 年 4 月以後，筑波，堂平，清澄等各地震観測所に設置中の無線地震計をつかい，Magnetic tape に集中録音された Data から遠地地震実体波並びに表面波について解析をおこなった．主な結果は次の通りである．

1) High-pass, Band-pass filtering は微弱な遠地地震初動の検出に有効である．

2) Low-pass filtering は短周期表面波，或は他の妨害波によって mask された長周期表面波の識別に有効である．

3) 一般に Analog filter を通した Data は Filter のもつ位相特性により位相偏位をうける．しかしこれらの Data に Double filtering method を適用することによって位相補償をおこなうことができる．

4) 地震波動実体波のスペクトル構造をしらべるため Multi-channel Band-pass filter をもちいた．

46 ケの遠地地震について解析をおこない，得られた結果から主として Magnitude と P 波の卓越周期の関係についてしらべた．一般に Magnitude の増加にしたがって卓越周期が大きくなる傾向にある．しかしその関係は一様ではなく，たとえば同じ Magnitude range においてもその値は大きく異なり，多分に地震の発生する地域の影響をうけるものと考えられ，引続き研究を続ける予定である．
